

# Evaluation of the new dynamic needle penetrometer in estimating uniaxial compressive strength of weak rocks

Pedram Azadan · Kaveh Ahangari

Received: 12 May 2012 / Accepted: 15 March 2013 / Published online: 9 April 2013  
© Saudi Society for Geosciences 2013

**Abstract** Studying the mechanical characteristics of weak sedimentary rocks is a burning issue in civil and mining engineering designs and analysis since obtaining rock mechanical properties of these has always faced lots of problems and uncertainties due to the structural weaknesses. One of the main causes of these problems is the difficulty of preparing high-quality core specimens recommended by testing standards or suggested methods for uniaxial compressive strength (UCS). For resolving this issue, in this study, common methods for indirect estimation of UCS of weak rocks were initially studied, their merits and demerits were analyzed, and then, in light of their positive and negative points, a new modified device was designed with a different mechanical structure and force exertion system, which could be practically used to present a new method for indirect estimation of UCS. Thus, in this study, we initially had a general view of the new dynamic needle penetrometer and its modified parts and their capabilities. After introduction, as the first phase of the practical studies on this, dynamic needle penetration resistance (DNPR) was measured, as the dynamic needle penetrometer test result, from 65 specimens collected from three different projects. Then, the relationships between DNPR and UCS of the rock specimens and the regressions of correlations were statistically analyzed. Finally, a linear equation with considerable accuracy resulted from analysis, and using this led to solving the main problem of this research by proposing a developed method for indirect estimation of uniaxial compressive strength of weak rocks.

**Keywords** Dynamic needle penetration resistance · Needle penetrometer · Uniaxial compressive strength · Weak rocks

## Introduction

Sedimentary rocks make up the major parts (about 70 %) of rocks in geological formations. More than 60 % of these rocks are weak and contain clay minerals (Potter et al. 1980; Saket 2006). This is also true for the geological formations in Iran (Saket 2006). Civil and mining projects are no exceptions, and one is likely to confront sedimentary rocks in lots of these projects. Due to the structural weaknesses of these rocks and sensitivity of their clay minerals to humidity, in these projects, weak rocks may cause a number of problems, especially in the presence of humidity. Therefore, if these rocks exist in either civil or mining projects, gathering acceptable range of data as to the structure of the rocks and their mechanical characteristics would be critical, especially in prefeasibility and feasibility studies since studying, designing, and performing the project should be done regarding this fundamental information in order to reduce the potential problems, which might arise if the characteristics of these types of rocks are overlooked. However, there are serious difficulties in obtaining rock mechanical properties of some sedimentary rocks. For overcoming these and preventing serious failures in projects, Gokceoglu and Aksoy (2000) introduced new approaches to the characterization of these rock masses by the inclusion of new parameters in the modified rock mass classification (M-RMR).

When sedimentary rocks with clay minerals (such as Montmorillonite) absorb humidity, they will be subjected to a serious structural weakness or even slaking (Gokceoglu et al. 2000). It could also be a serious problem for measuring mechanical properties of these rocks because of the high-quality core specimens recommended by testing standards or

---

P. Azadan · K. Ahangari (✉)  
Department of Mining Engineering, Science and Research Branch,  
Islamic Azad University, Tehran, Iran  
e-mail: kaveh.ahangari@gmail.com

P. Azadan  
e-mail: pedramazadan@hotmail.com

suggested methods for uniaxial compressive strength (UCS), so determinations cannot always be obtained, particularly from weak, thinly bedded, and clay-bearing rocks. In view of this difficulty, some modeling methods and also some simple index test methods such as point load, Schmidt hammer, and block punch index (BPI) tests have been developed in order to indirectly estimate the UCS (Ulusay and Gokceoglu 1997). For instance, Minaeian and Ahangari (2011) proposed a new linear correlation between UCS and the rebound value of the Schmidt hammer by testing 70 specimens of weak rocks collected from different formations in Iran with satisfying regression of 0.935 (Eq. 1). Cevic et al. (2011) also documented the results of laboratory experiments and numerical simulations (i.e., neural network) conducted to estimate the uniaxial compressive strength of some clay-bearing rocks selected from Turkey, and the NN models developed in the study provided a very high performance as well.

$$\text{UCS} = 0.678 R_L \quad (1)$$

However, preparation of small specimens from such rocks for some of these simple index tests like BPI and point load could sometimes be difficult (Erguler and Ulusay 2009). For resolving this issue, new nondestructive portable testing devices called needle penetrometers have been developed by manufacturers in Japan and the Netherlands. These devices measure the needle penetration resistance (NPR) of weak and soft rocks both in field and in laboratory (Ulusay and Erguler 2007; Aydan et al. 2008; Erguler and Ulusay 2009; Ngan-Tillard et al. 2009; Ngan-Tillard et al. 2011, 2012). These penetrometers are common devices for estimating UCS of weak rocks, and lots of studies have been published about them thus far. Using penetrometers for geotechnical studies started from pocket penetrometers. They were introduced and used in the 1970s for indirect estimation of compressive strength of weak and uniform soils. One of the most important advantages of these devices was their direct indication of compressive strength. Therefore, researchers warmed to use them more and more. Even now, after a few decades, pocket penetrometers are still used for indirect estimation of compressive strength of soils which have strength less than 4.5 kg/cm<sup>2</sup> in some projects (Humboldt Co. 2003).

Later, in 2006, Maruto Corporation from Japan introduced the compressive needle penetrometer for indirect estimation of the uniaxial compressive strength of weak rocks. This device was used in several studies and showed good results for weak rocks. The major difference between this device and the pocket penetrometer was that the estimated strength was not shown directly in this instrument. Instead, a constant was defined called needle penetration resistance (NPR). NPR index was obtained by dividing the exerted force in newton (N) by the penetration rate in millimeter, both of which were shown on the indicators.

The load indicator scaled between 10 and 100 N with graduation of 10 N and penetration rate indicated from 1 to 10 mm with 1 mm graduation. By putting NPR in an equation, UCS has been estimated (Maruto Co. 2006; Ulusay and Erguler 2007; Erguler and Ulusay 2009). The following empirical relationship with a high coefficient of correlation ( $r=0.87$ ) between the UCS and NPR was introduced by Erguler and Ulusay (2009):

$$\text{UCS} = 0.51(\text{NPR})^{0.8575} \quad (2)$$

The other needle penetrometer used for estimating UCS is the equipment manufactured by Eijkelkamp in the Netherlands. Due to the application for estimation of the UCS of very weak to weak rocks, the standard Eijkelkamp cone has been replaced by a short needle made of hardened steel, and needles with a diameter of 1 or 1.4 mm and with a flat or a conical tip are available. It should be noted that their conical part, if any, is less than 1.3 mm long while the shaft of the Maruto needle increases slowly from 0 to 0.84 mm in diameter over about 10 mm. The needle of the Eijkelkamp

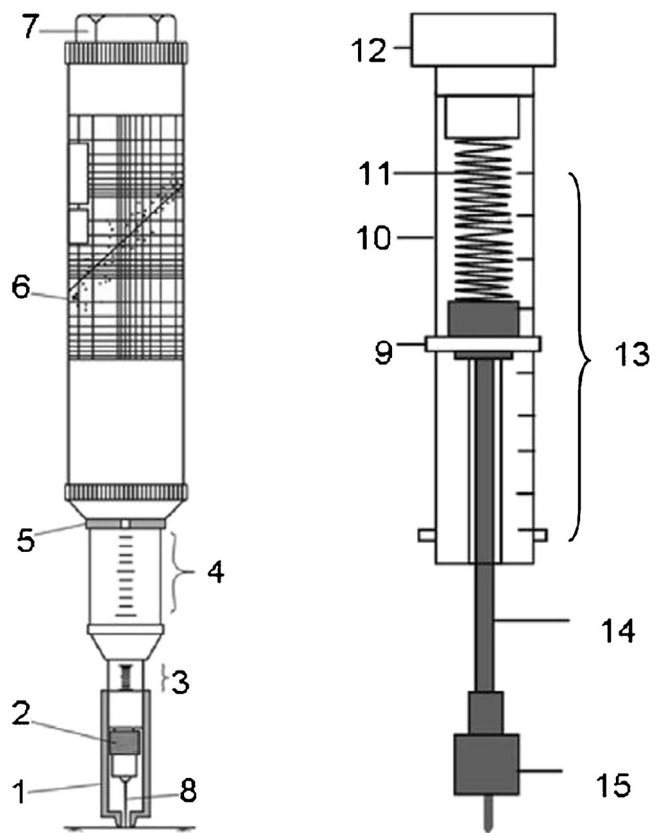


**Fig. 1** General view of the Maruto (*left*, from Maruto Co. 2006) and modified Eijkelkamp (*right*, from Ngan-Tillard et al. 2011) penetrometers and their parts. 1 presser, 2 chuck, 3 penetration, 4 load scale, 5 load indication ring, 6 UCS–NPR correlation chart given by the manufacturer, 7 removable cap, 8 penetration needle produced according to the Japan Civil Engineering Society's guideline, 9 indicator ring, 10 penetrometer tube, 11 spring, 12 end cap, 13 scale, 14 extension rod, and 15 needle block

penetrometer is pushed until a constant compression of the spring is observed or the maximum needle penetration (8.5 mm) is reached. The spring compression is read with the help of an indicator ring on the millimeter scale of the penetrometer. The maximum spring compression is 8.5 cm. Like cone tip resistance, the needle resistance, NPRES, is calculated by multiplying the spring stiffness by the observed spring compression and by dividing the calculated force by the needle cross section. The sensitivity of the Eijkelkamp penetrometer can be optimized by adjusting the spring stiffness. Springs with a capacity of 50, 100, and 150 N are available. In contrast with the Maruto penetrometer, the Eijkelkamp penetrometer does not allow the simultaneous measurement of the load and penetration depth (Ngan-Tillard et al. 2009, 2011). The Maruto penetrometer and modified Eijkelkamp penetrometer's general views (Maruto Co. 2006; Ngan-Tillard et al. 2011) have been presented in Fig. 1.

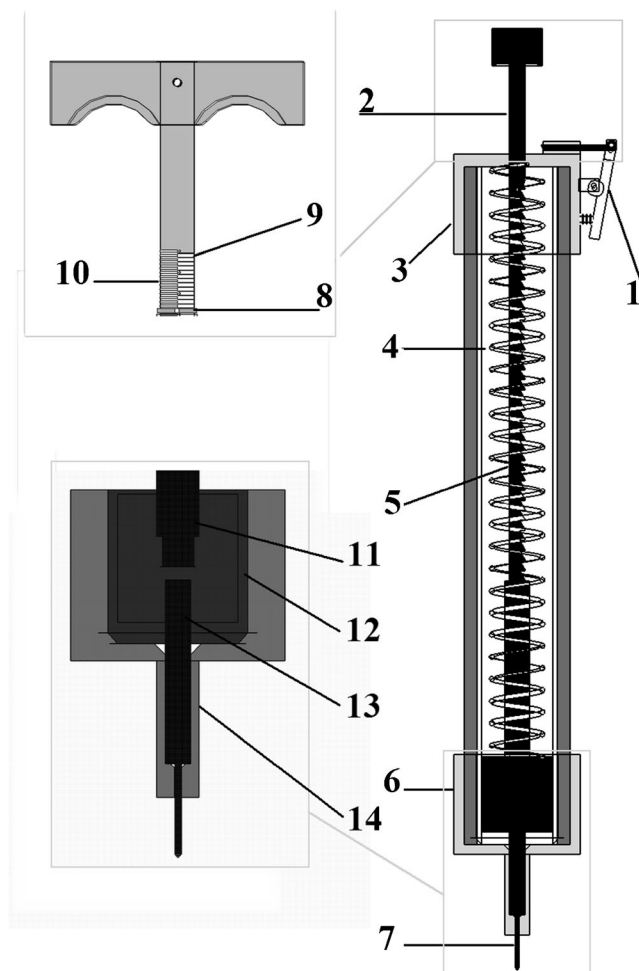


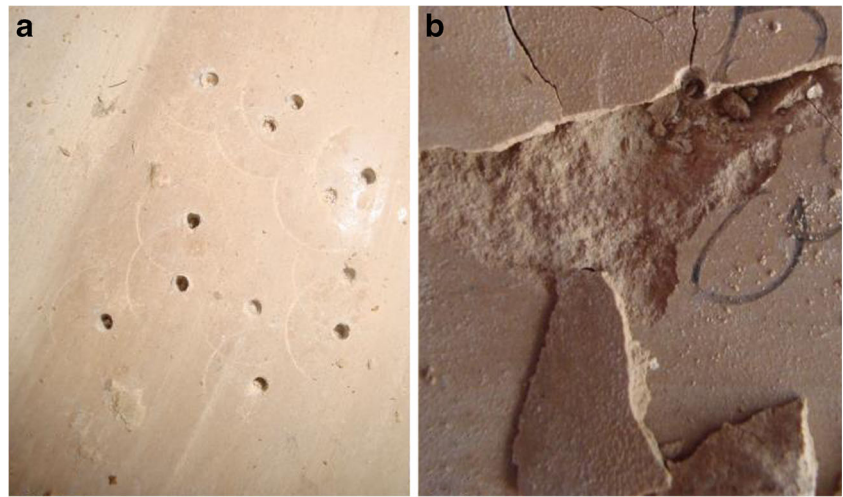
**Fig. 2** General view of the dynamic needle penetrometer and its parts. 1 trigger, 2 rod, 3 removable cap, 4 spring, 5 reinforcement indicators (1~40), 6 end cap, 7 needle, 8 indicator ring, 9 penetration indicator (0.5~14.5 mm), 10 penetration indicator (0~15 mm), 11 rod, 12 piston, 13 needle, 14 needle guide

The needle penetrometer test was successfully used by Ngan-Tillard (2011) to distinguish qualitatively carbonate sands from very weak and weak calcarenites in borehole cores recovered for cut-and-cover tunnel projects in Maastricht. Then, the relation between UCS and needle penetration resistance (NPR) for the Maastrichtian limestones was further analyzed. Results from the study suggest that there is a statistically significant relationship between the UCS and NPR for 78 datasets of UCS and NPRES with



**Fig. 3** Two different views of the 3D model of the dynamic needle penetrometer: a the assembled view, b the bare view

**Fig. 4** Effect of different shapes of the needle tip on the specimens in dynamic needle penetration test. **a** 60° conical tip, **b** hemispherical tip



an  $r$  of 0.834 that leaves, however, too high predictive uncertainty (Eq. 3).

$$\text{UCS} = 0.0731 \text{ DNPR}_E \quad (3)$$

During testing with the Eijkelpamp penetrometer, very high compressive and shear stresses develop under the needle and stresses normal to the needle shaft increase, but no trend in the maximum resistance was visible as a function of needle geometry and size (this result was considered in the designing of the new dynamic penetrometer). Nevertheless, resistance to needle penetration and UCS values are somehow related, but the needle penetrometer was recommended as an index test rather than a way to determine accurately the UCS of the Maastrichtian limestones (Ngan-Tillard et al. 2009, 2011).

Although the needle penetrometer (NP) is a cheap and practical device for estimating UCS, it has some disadvantages as well. The most important disadvantages of the NP are its static force exertion system, its reliance on hand pressing, 10 N and 1 mm graduation of the device indicators (Maruto Co. 2006), and its high predictive uncertainty in field studies (Ngan-Tillard et al. 2011). In light of these disadvantages, the dynamic needle penetrometer (DNP) has been designed with different mechanical structures and modified for application on the surface of weak rocks both in field studies and in laboratories to determine dynamic needle penetrometer resistance (DNPR). After a review on the new dynamic penetrometer mechanical properties, its modified parts, and materials used for producing it, the ability of DNP in estimation of the weak rocks' UCS has been examined by statistically analyzing the relation between UCS and DNPR in this study. Along with

these tests, the effect of density has been studied as an important and effective factor on the results of the tests, and the performance of the DNP is also compared with the results obtained drawing on the Schmidt hammer and point load test.

### Designing the new dynamic needle penetrometer

Given the aforementioned information, a needle penetrometer was designed with a dynamic force exertion system in order to present a new method for indirect estimation of mechanical properties of weak rocks. The dynamic needle penetrometer is a new kind of penetrometer in which the force exertion system is not static (unlike the previous models) and results from the impact force of spring reinforcement (just like what happens in the Schmidt hammer). Nevertheless, unlike the Schmidt hammer, the maximum spring compression in the DNP is 18.75 cm, and it also has 40 different rates of impact force exertion for different rocks ranging from soft to very soft. Thanks to this special design, this can be applied into a wide variety of weak and very weak rocks. In Fig. 2, a general view of the DNP with its parts is presented. In addition, to clarify, Fig. 3 presents two different views (assembled and bare views) of the 3D model of the DNP.

Almost all the parts of this device are made up of stainless steel A304 (ASTM 2011) for improving its rigidity in different climates and also in case of falling down from a height during the field studies, but chrome vanadium A231 (ASTM 2010) is used for building its spring because these alloy spring steels have a definite place in the field of spring materials,

**Table 1** Descriptive specifications of UCS and DNPR parameters obtained from samples of Siah Shir dam

Parameter	Qt.	Range	Minimum	Maximum	Mean	Std. deviation	Variance	Kurtosis	Skewness
UCS (MPa)	15	5.69	14.91	20.60	17.38	1.76268	3.107	-0.608	0.208
DNPR (N/mm)	15	5.32	11.11	16.43	13.89	1.77770	3.160	-1.272	0.291

**Table 2** Descriptive specifications of UCS and DNPR parameters obtained from samples of Tang Sorkh dam

Parameter	Qt.	Range	Minimum	Maximum	Mean	Std. deviation	Variance	Kurtosis	Skewness
UCS (MPa)	38	23.60	16.20	39.80	29.31	6.34837	40.302	-0.684	0.514
DNPR (N/mm)	38	20.61	12.40	33.01	23.87	4.97494	24.750	-0.681	0.482

particularly for conditions involving high stress and for applications where shock or impact loading occurs. Furthermore, crucible tool steel S-7 (ASTM A681 2008) was selected for producing the needles since it possesses high toughness and shock resistance. Although it does not have hardness comparable to the other tool steels (Rockwell 56C), S7 is very tough compared to other tool steels. Thus, using it significantly decreases the number of broken needles during the tests and leads to more accuracy in results as well.

Another important change in the DNP is the new penetration depth indication system. According to its mechanical design, linear relocation of the needle (penetration rate) is equal to linear relocation of the whole parts attached to the rod from the needle and piston to the handle, so the indicator system has been located on the upper part of the rod and under the handle, and it can indicate the penetrations from 0.5 to 15 mm. It can indicate depth of penetration with a resolution of 0.5 mm by its mechanical indicator, which is more accurate than previous devices like the Maruto needle penetrometer with a resolution of 1 mm (Fig. 2). Furthermore, thanks to this structure, linear encoders can be used for obtaining more accurate penetration rates from relocation of the handle instead of the mechanical indicator systems as well. Therefore, a digital caliper with a resolution of 0.01 mm was used rather than the mechanical indicator of the penetrometer to improve the accuracy of the DNPR values that resulted in the laboratory. The penetrator part of the DNP is a needle which is 1.5 mm in diameter. This diameter was selected from needles with 1-, 1.5-, and 2-mm diameter, all made from S-7 tool steel with hardness of 56 C Rockwell after testing them on the surface of five uniform mudstone specimens. In this selection, brittleness of the needles and ability of penetration were considered. In addition to the diameter, studying the penetration ability of flat, hemispherical, 60° cone, and 90° cone tips on the surface of the rock specimens was also done. Finally, considering the performance of different needles, the 60° cone-shaped needle tip was selected because it wreaked less destruction on the surface of the specimens (Fig. 4). After these modifications, the DNP is ready for testing in the field or laboratory.

In order to use this penetrometer either in field or laboratory tests, first, it should be reinforced according to the structural strength of the specimens, and then, the impact force is exerted. Next, the penetrating rate is read from the mechanical or digital penetration indicator (Fig. 2, left, mechanical indicator). This test is carried out three to ten times in different force exertion levels, and the penetration rate and the force exertion level are recorded. DNPR is measured by dividing the defined force for the force exertion level exerted ( $F$ ) in newton, which is introduced based on multiplying the stiffness of the spring ( $K$ ) by its compression, by the penetration depth ( $P$ ) in millimeter.

$$\text{DNPR} = \frac{F}{P} \quad (4)$$

It is necessary to describe the reason for using the defined forces for the levels of reinforcement. As the dynamic impact force is different when exerted to the surface of the different materials, it is needed to use a defined and fixed force for each level of reinforcement. The DNP test does not require special shape of specimen, and it could be introduced as an advantage of this in comparison with some tests like BPI and point load. Moreover, another important positive point about this device is its low production cost as economic viability has been accounted for in its designing.

In the next section, the new device is practically used in the DNP test, and the relationship between DNPR and UCS is statistically analyzed for finding an equation in order to indirectly estimate the UCS of weak rocks.

### Experimental procedures

In this research, the practical use of the needle penetrometer with dynamic force exertion system is mainly discussed. Thus, for the first phase of examining the DNP, in this study, rock specimens from different formations in Iran had to be selected, so a number of samples were collected from Siah Shir earth dam, Tang Sorkh reservoir dam, and Tang Tizab water diversion tunnel. In the selection of these specimens, in order to

**Table 3** Descriptive specifications of UCS and DNPR parameters obtained from samples of Tang Tizab tunnel

Parameter	Qt.	Range	Minimum	Maximum	Mean	Std. deviation	Variance	Kurtosis	Skewness
UCS (MPa)	12	26.30	13.70	40.00	31.39	9.96594	99.320	-0.861	-0.923
DNPR (N/mm)	12	23.86	10.16	34.02	26.20	8.58321	73.672	-0.406	-1.072

**Table 4** Descriptive specifications of UCS and DNPR parameters obtained from all of the samples in this study

Parameter	Qt.	Range	Minimum	Maximum	Mean	Std. deviation	Variance	Kurtosis	Skewness
UCS (MPa)	65	26.30	13.70	40.00	26.945	8.336	69.496	-0.016	-1.469
DNPR (N/mm)	65	23.86	10.16	34.02	21.997	6.961	48.457	-0.040	-1.350

study the relationship between UCS test and DNPR, the capability of performing the UCS test was considered since accurate UCS results were needed to propose a valid and acceptable equation. Finally, in view of this factor and because of the sensitivity of some specimens to humidity, 65 specimens were selected, and only dry ones were used for the tests, so all the specimens were dried in a ventilated oven at 105 °C for at least 24 h, and all tests were carried out on them to prevent slaking. In the next four sections, some data about the specimens and the test results of each of these three projects will be presented separately, and then all results will be analyzed collectively.

#### Siah Shir earth dam

This site is located in Siah Shir region, south of the town of Bahmaei in the provinces of Kohkilooyeh and Boyerahmad. In this research, 15 specimens, constituting mudstones and sandstones of the Bakhtiari formation, were used with an average dry density of 1.9206 kg/cm<sup>2</sup>. The Bakhtiari is the youngest formation in the Zagros area, which consists of conglomerates, sandstones, and mudstones (Ismail and Al-Juboury 2009). The UCS test of each specimen was performed according to the International Society for Rock Mechanics (ISRM) suggested methods (2007). The results were between 14.91 and 20.6 MPa.

After performing UCS test on each specimen, DNP test was done by the new dynamic penetrometer three to ten times on another part of the same specimen that was prepared and dried for DNP test. Then, the mean of obtained DNPR results was considered as the DNPR (in newton per millimeter) of the specimens. In Table 1, descriptive characteristics of all results from UCS and DNP tests on the specimens of Siah Shir are shown. In addition to these, Schmidt hammer type L rebound value ( $R_L$ ), regarding the Aydin and ISRM suggested method (2008), was obtained for all the specimens. The point load standard index ( $I_s(50)$ ) of the specimens, which had a UCS of 15 MPa or higher measured according to the ASTM D5731 standard (2008), was also obtained. Macroscopic descriptions, specimen number, depth of sampling, dry density, porosity, water absorption, UCS, DNPR,  $R_L$ , and  $I_s(50)$  of the specimens are shown in Table 8 (Appendix).

#### Tang Sorkh reservoir dam

This project is situated near Hassan Abad village, 35 km onto the Yasooj-Shiraz road. This dam is in the Gurpi formation, which is one of the formations located in Fars province. This formation consists of marl, shale, and limestone. The major difference between the rocks of this formation and the rocks of Gachsaran formation is the lack of

**Fig. 5** Normal curve and histogram of UCS and DNPR parameters

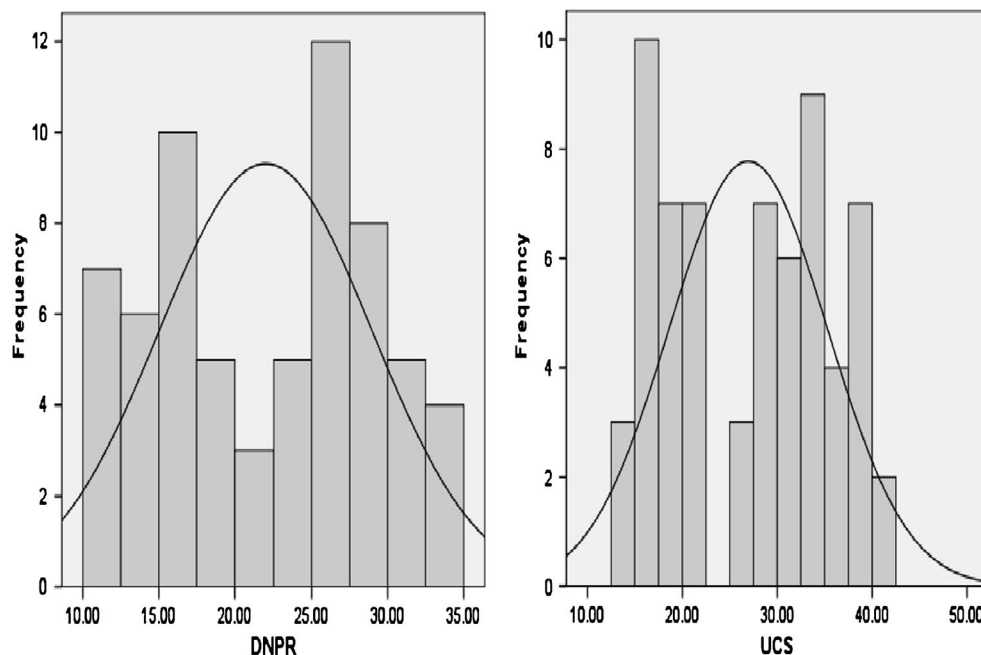


**Table 5** Obtained linear equations between UCS and DNPR

Equation	$R^2$	$F$	Parameter	$t$	Sig.	Type	Eq. no.
$UCS = 1.219DNPR$	0.994	1.154E4	DNPR	107.405	0.000	Without intercept	(5)
$UCS = 1.16DNPR + 1.423$	0.939	962.994	DNPR $C$	31.032 1.651	0.000 0.104	With intercept	(6)

salt and anhydrite in the Gurpi formation (Bahrami 2010; Tavakoli-Shirazi et al. 2012).

Thirty-eight specimens of marl, limestone, and shaley and marly limestones were selected from this project with an average dry density of 2.4910 kg/cm<sup>2</sup>. The results of UCS test on these specimens range from 16.20 to 39.80 MPa. Obtaining the DNPR of the specimens from Tang Sorkh dam with the UCS of near 40 MPa posed some problems, so the specimens with the UCS of more than 40 MPa were not tested. There were two main reasons for such difficulties. The first reason was the necessity of increasing force exertion as well as the increase of specimen penetration resistance, which could lead to less accurate results because of some factors like meager depth of penetration. The second one was the increase of probability of needle breakage due to the increase of the surface resistance and brittleness of some specimens. Descriptive characteristics of all data resulting from UCS and DNPR tests done on the specimens of Tang Sorkh dam are shown in Table 2. Moreover, two additional indexes, i.e.,  $R_L$  and  $I_s(50)$ , were measured for all specimens of this project, like the previous group of specimens. Macroscopic characteristics and other results and information about Tang Sorkh specimens were presented in Table 9 in detail (Appendix ).

Tang Tizab water diversion tunnel

This tunnel is located between two valleys of Rokouh Torbakestan and Chahar Maroon near the town of Sepidan. Although the formation of this region is Gurpi just like the formation of the Tang Sorkh project, the specimens of this region were mostly cores, which were obtained from the drilling operation at a greater depth in comparison with the Tang Sorkh project. The specimens consisted of limestone and marly limestone that were darker and somehow stronger than the specimens from the Tang Sorkh project.

Considering the mentioned characteristics of the specimens and also practical experiences gained from specimens of Tang Sorkh, only the specimens with UCS of 40 MPa or under were examined in order to prevent the high rate of needle breakage during the DNP test. Therefore, among specimens from the Tang Tizab project, only 12 specimens were chosen with an average dry density of 2.3633 kg/cm<sup>2</sup> and the UCSs from 13.7 to 40 MPa. DNP test was done on these specimens, too. In Table 3, descriptive characteristics of the Tang Tizab specimens are shown, and more information about these specimens and test results, with obtained  $R_L$  of all specimens and  $I_s(50)$  of suitable specimens (UCS, 15 MPa or more), is presented in Table 10 (Appendix).

**Data analysis**

After obtaining two datasets of UCS and DNPR from 65 specimens with an average dry density of 2.3370 kg/cm<sup>2</sup>, the results were analyzed collectively. Descriptive characteristics of UCS and DNPR for all specimens are shown in Table 4. The normal curve and histogram of this collection are shown in Fig. 5. Although there are slightly log-normal distributions, which spring from unpredictable behavior of different types of rocks from different formations and rock masses, the normal curves reveal a significant statistical correlation between the parameters. Additionally, the amount of kurtosis and skewness of both sets are almost the same, showing a relatively normal and acceptable distribution. This similarity helps to increase the accuracy of statistical equations between two datasets. One of the common methods to establish a predictive equation among the relevant parameters of rocks in rock engineering is regression analysis. Thus, in this study, this method was used by employing 12 different kinds of correlations (Eqs. 5–16), and then obtained regressions and  $F$  values of them were analyzed. The results are presented in Tables 5, 6, 7.

**Table 6** Obtained non-linear equations between UCS and DNPR with intercept

Equation	$R^2$	$F$	Sig.	Type	Eq. no.
$UCS = 1.506(DNPR)^{0.933}$	0.937	940.021	0.000	Power	(7)
$UCS = e^{0.046(DNPR)+2.24}$	0.931	853.907	0.000	Exponential	(8)
$UCS = 23.397Ln(DNPR) - 44.102$	0.917	700.502	0.000	Logarithmic	(9)
$UCS = e^{\frac{-17.184}{DNPR} + 4.118}$	0.905	598.463	0.000	S	(10)
$UCS = \frac{-424.546}{DNPR} + 48.562$	0.860	386.304	0.000	Inverse	(11)

**Table 7** Obtained non-linear equations between UCS and DNPR without intercept

Equation	$R^2$	$F$	Sig.	Type	Eq. no.
$UCS = (DNPR)^{1.066}$	0.999	7.762E4	0.000	Power	(12)
$UCS = e^{0.138(DNPR)}$	0.957	1.422E3	0.000	Exponential	(13)
$UCS = 9.052Ln(DNPR)$	0.963	1.657E3	0.000	Logarithmic	(14)
$UCS = e^{\frac{54.642}{DNPR}}$	0.821	292.634	0.000	S	(15)
$UCS = \frac{54.642}{DNPR}$	0.656	122.044	0.000	Inverse	(16)

Comparing  $R^2$  (regression squared) of equations showed that Eqs. 5 and 12 had higher regressions and accuracies compared to the others. Eq. 12 (power equation without intercept) had a  $R^2$  of 0.999, and it showed the highest regression and accuracy, followed by Eq. 5 (linear equation without intercept) with  $R^2$  of 0.994. However, using linear equations is usually more reliable and preferred to other methods because of the simplicity of calculation, so Eq. 5 in Table 5 was selected in this study.

$$UCS = 1.219 DNPR \tag{5}$$

The figures for three projects are compared in the diagram of Fig. 6. The points should be on the equation line slope for a perfect estimation and on lines with 1:0.5 and 1:2 slopes when the estimation is twice or half as much as the obtained UCS value, respectively. Reviewing Fig. 6 offers a more accurate picture of the effect of increasing UCS on reducing the accuracy of the estimation. Besides, it is obvious that most data, which are far from the line of the selected linear equation, were obtained from the specimens of Tang Sorkh dam since testing these specimens raised some problems due to their high brittleness. Furthermore, the comparison of average dry densities of each project gives essential information about this problem. It shows that increasing the density might adversely affect the DNP tests. For example, specimens from the Tang Sorkh caused more difficulties in the DNP test and also had more

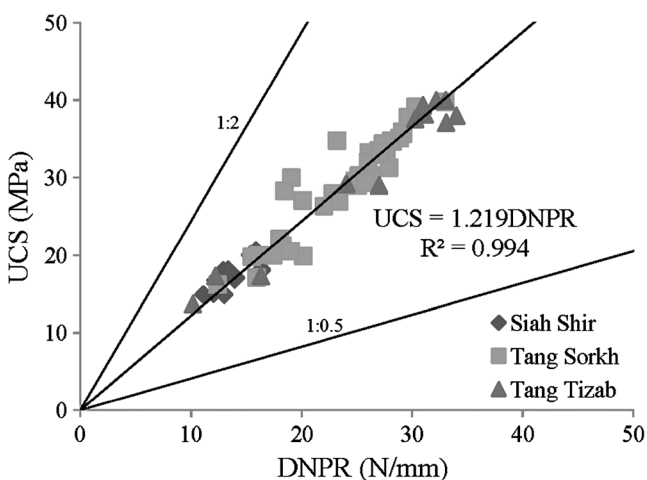


**Fig. 6** The graph of linear equation between DNPR and UCS

average density than the others, while it was quite the opposite with regard to the Siah Shir project. Putting all these together, most of the points fall very close to the equation line, indicating a general agreement between the predicted and measured UCS values, and meet the expectations, enabling the new method to be used for indirect estimation of UCS of very weak to weak sedimentary rocks (UCS, 40 MPa or under).

To illustrate, the accuracy of the DNP method in this study, in addition to the introduced method, UCSs of specimens were also estimated by two other common index methods regarding the measured indexes of the samples (Appendix, Tables 8, 9, and 10). For the prediction of the UCS from the Schmidt hammer values, Eq. 1 (Minaeian and Ahangari 2011) was used, and estimated strengths resulting from point load index were obtained according to the related standard suggestions (ASTM D5731 2008). Predicted UCSs were estimated by using three different index methods: Schmidt hammer, point load, and the DNP, which are compared in Fig. 7. It can be clearly seen that in this research, the prediction of the DNP is by far the most accurate one, followed by point load test and Schmidt hammer, which provide significantly further results from the line 1:1. It is also considerable that in this study, estimation of the point load test is far more accurate for samples with UCSs of more than 30 MPa.

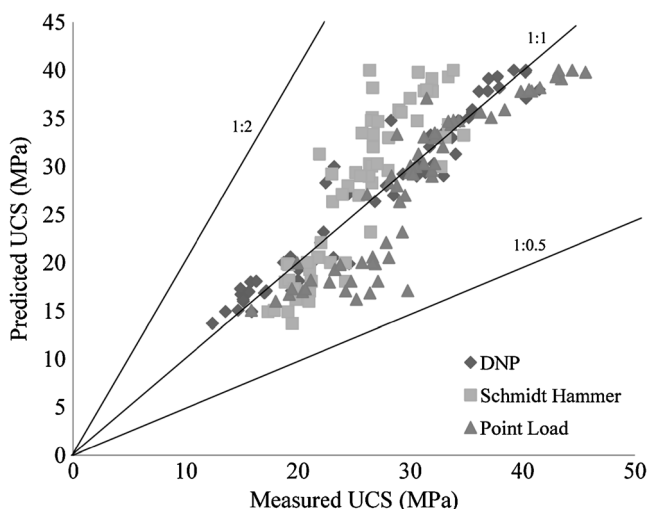


**Fig. 7** Comparison between measured UCSs and UCSs estimated by three different index methods



## Conclusions

The conclusions drawn from this study are summarized as follows:

- The dynamic penetrometer is a new device to solve the main problem of this research due to its benefits such as the capability of dynamic force exertion in 40 different levels, more accurate penetration indicating systems, and, of course, its ability to be used in both field studies and laboratory tests.
- The first practical use of the dynamic penetrometer showed the capability of performing tests on the specimens with UCS of 40 MPa or under, and it could be an acceptable range for these kinds of devices.
- The obtained dry densities in this study showed that the increasing of density might decrease the accuracy of DNP tests.
- The regression analysis among correlations between UCS and DNPR parameters resulted in a selected linear equation ( $R^2=0.994$ ), which showed a satisfactory level

of accuracy. This equation could resolve the burning issue of estimating weak rock characteristics and proved that the introduced index method for weak rocks is applicable.

- Comparison between three different estimated values for UCS, resulting from Schmidt hammer, point load, and dynamic needle penetrometer, showed that the predictions of the DNP were obviously more accurate in this study.

Despite the fact that the DNP shows these merits in this study, the ability of this device to estimate UCS was only examined in the first phase of studies and on a limited number of selected uniform specimens, so it needs more studies on different specimens from different kinds of rocks with different mechanical properties for accepting DNPR as a reliable index to use widely in field studies. Moreover, it could be beneficial to study the effects of other characteristics of rocks and rock masses on the DNPR, and also to compare the DNP test with NP tests in future studies.

## Appendix

Additional information about 65 rock samples

**Table 8** Macroscopic description, depth, type, dry density, porosity ( $n$ ), water absorption ( $A_w$ ), DNPR, UCS, Schmidt hammer rebound, and point load index of Siah Shir dam samples

Sample no.	Sample serial	Rock type	Macroscopic description	Depth (m)	Density (kg/cm <sup>3</sup> )	$n$ (%)	$A_w$ (%)	UCS (MPa)	DNPR (N/mm)	$R_L$	$I_s(50)$ (MPa)
1	b-1-03	Sandstone	Fine-grained light brown sandstone with inter layers of mudstone	25.35 to 26.05	1.92	9.07	4.30	17.07	14.080	31.01	1.01
2	b-1-04	Sandstone	Same as above	26.65 to 27.10	1.93	9.07	4.32	16.86	13.948	30.21	1.10
3	b-1-05	Sandstone	Same as above	27.10 to 27.60	1.93	7.00	3.30	20.03	15.341	33.73	1.07
4	b-1-06	Sandstone	Same as above	32.00 to 32.45	2.04	9.30	4.45	20.60	15.848	32.28	1.11
5	b-1-07	Sandstone	Same as above	32.45 to 32.90	1.95	6.23	2.90	18.08	16.425	35.78	1.03
6	b-2-01	Mudstone	Faintly weathered, moderately jointed brown mudstone	9.50 to 10.00	1.83	12.13	5.75	14.91	13.022	28.17	–
7	b-2-02	Mudstone	Same as above	11.00 to 11.50	1.88	9.33	4.34	18.00	12.950	27.81	0.95
8	b-2-03	Mudstone	Moderately jointed brown mudstone	13.35 to 14.00	1.83	10.92	5.15	16.00	12.418	30.91	0.75
9	b-2-04	Mudstone	Weathered, brown mudstone	18.45 to 19.00	1.87	12.81	6.10	14.92	11.110	25.56	–
10	b-2-05	Mudstone	Same as above	19.10 to 19.55	1.89	12.40	5.98	15.06	12.030	26.38	0.66
11	b-3-08	Sandstone	Faintly weathered, fine-grained sandstone with interlayers of mudstone	28.75 to 29.25	1.92	6.30	2.85	16.72	12.244	29.32	0.80
12	b-3-09	Sandstone	Same as above	34.00 to 34.60	2.02	6.90	3.15	18.08	13.351	31.21	1.13
13	b-4-01	Mudstone	Weathered brown mudstone with interlayers of sandstone	12.40 to 12.70	1.92	9.07	4.30	17.00	12.820	21.69	0.85
14	b-4-02	Mudstone	Faintly weathered brown mudstone	18.45 to 19.00	1.90	7.88	3.70	18.20	16.392	28.28	0.88
15	b-4-03	Mudstone	Weathered, jointed brown mudstone with interlayers of sandstone	20.00 to 20.45	1.98	9.40	4.50	19.30	16.415	31.03	0.97

**Table 9** Macroscopic description, depth, type, dry density, porosity ( $n$ ), water absorption ( $A_w$ ), DNPR, UCS, Schmidt hammer rebound, and point load index of Tang Sorkh dam samples

Sample no.	Sample serial	Rock type	Sample description	Depth (m)	Density (kg/cm <sup>3</sup> )	$n$ (%)	$A_w$ (%)	UCS (MPa)	DNPR (N/mm)	$R_L$	$I_s(50)$ (MPa)
16	2-1-03	Marly limestone	Weathered, gray marly limestone with open joints that filled by silt and clay	17.00 to 17.45	2.37	4.45	1.80	20.00	17.456	35.73	0.83
17	2-1-06	Marly limestone	Dark gray marly limestone	32.88 to 33.40	2.49	4.18	1.68	30.00	19.049	48.27	1.27
18	2-1-07	Marly limestone	Marly limestone	36.67 to 37.00	2.48	4.27	1.72	27.00	23.385	37.49	1.23
19	2-1-08	Marly limestone	Gray marly limestone	41.20 to 41.75	2.47	4.59	1.86	28.00	22.861	36.07	1.20
20	2-2-01	Marl	Moderately jointed brownish gray marl	10.12 to 10.57	2.37	6.75	2.85	16.20	12.399	29.21	1.05
21	2-2-02	Marly limestone	Moderately jointed, brownish gray marly limestone	18.50 to 18.90	2.41	6.29	2.61	19.90	20.155	28.07	1.12
22	2-2-04	Marl	Weathered gray marl	32.90 to 33.27	2.50	6.55	2.75	33.27	26.080	51.29	1.35
23	2-2-11	Marly limestone	Fresh, moderately jointed, brownish gray limestone to marly limestone	61.60 to 62.00	2.49	4.44	1.79	26.36	22.022	34.07	1.21
24	2-2-12	Limestone	Fresh, jointed gray limestone	68.32 to 68.60	2.47	4.67	1.89	28.30	18.430	39.21	1.17
25	2-2-15	Marly limestone	Dark gray marly limestone	76.00 to 76.50	2.49	4.43	1.78	30.30	25.201	38.91	1.30
26	2-3-01	Marly limestone	Weathered light brown to reddish marly limestone with open joints	7.75 to 8.20	2.40	6.39	2.66	22.10	18.033	32.51	1.16
27	2-3-02	Marly limestone	Reddish brown marly limestone	11.44 to 11.80	2.47	4.54	1.83	30.06	25.160	39.18	1.25
28	2-3-03	Marly limestone	Moderately weathered reddish brown marly limestone	19.35 to 19.80	2.53	6.52	2.73	27.10	20.069	35.31	1.09
29	2-3-05	Marly limestone	Same as above	26.35 to 26.78	2.39	4.54	1.83	17.10	15.937	29.39	1.24
30	2-3-07	Marly limestone	Fresh gray marly limestone	36.00 to 36.45	2.47	6.07	2.52	20.54	19.003	32.07	1.17
31	2-4-01	Marly limestone	Slightly weathered purple marly limestone	3.10 to 3.50	2.33	6.03	2.48	19.81	15.520	28.26	0.99
32	2-4-03	Marly limestone	Purple marly limestone	14.40 to 14.75	2.51	4.07	1.62	29.00	25.069	38.81	1.33
33	2-4-04	Marly limestone	Fresh purple marly limestone	17.18 to 17.75	2.51	4.68	1.88	32.05	26.010	39.38	1.37
34	2-4-05	Marly limestone	Purple marly limestone	21.35 to 21.75	2.52	3.88	1.54	29.60	24.820	41.32	1.33
35	2-4-06	Marly limestone	Fresh gray limestone	26.90 to 27.32	2.53	4.37	1.76	33.06	27.130	48.79	1.30
36	2-4-08	Limestone	Fresh gray limestone	36.33 to 36.78	2.54	4.25	1.70	23.20	18.262	39.04	1.22
37	2-7-01	Shaley limestone	Light gray shaley limestone	19.00 to 19.54	2.56	4.17	1.66	39.12	30.330	47.07	1.81
38	2-7-02	Shaley limestone	Fresh gray shaley limestone	21.00 to 21.40	2.54	3.74	1.48	34.76	28.114	45.14	1.43
39	2-7-04	Shaley limestone	Fresh light gray shaley limestone	32.60 to 33.00	2.52	3.93	1.56	34.38	27.352	49.25	1.40
40	2-7-06	Shaley limestone	Dark gray shaley limestone	40.20 to 40.75	2.54	3.58	1.41	33.00	27.661	41.39	1.34
41	2-8-03	Shaley limestone	Weathered grayish purple shaley limestone	18.00 to 18.48	2.53	4.20	1.66	35.10	28.884	39.24	1.55
42	2-8-04	Limestone	Weathered grayish purple limestone	20.75 to 21.20	2.50	4.46	1.77	37.81	29.630	47.13	1.66
43	2-8-06	Limestone–shaley limestone	Dark gray alternation of limestone and shaley limestone with joints filled with crystals	34.15 to 34.55	2.52	4.56	1.81	34.80	23.206	39.15	1.41
44	2-8-10	Marly limestone	Fresh purple marly limestone	56.52 to 57.00	2.51	4.74	1.89	35.90	29.141	42.74	1.60
45	2-8-11	Shaley limestone	Fresh dark gray shaley limestone	62.00 to 62.45	2.54	3.71	1.46	39.80	33.008	45.28	1.90
46	G-1-02	Marly limestone	Weathered greenish gray marly limestone	12.25 to 12.75	2.53	4.15	1.64	34.70	28.252	39.99	1.39
47	G-1-03	Marly limestone	Same as above	23.00 to 23.60	2.54	3.84	1.52	35.66	29.147	43.03	1.51
48	G-1-06	Marly limestone	Gray marly limestone	33.85 to 34.25	2.53	4.07	1.61	30.30	26.320	39.91	1.34
49	G-1-07	Marly limestone	Fresh, faintly weathered gray marly limestone	46.50 to 46.83	2.49	3.57	1.40	20.03	16.126	30.71	1.11

**Table 9** (continued)

Sample no.	Sample serial	Rock type	Sample description	Depth (m)	Density (kg/cm <sup>3</sup> )	<i>n</i> (%)	<i>A<sub>w</sub></i> (%)	UCS (MPa)	DNPR (N/mm)	<i>R<sub>L</sub></i>	<i>I<sub>s</sub></i> (50) (MPa)
50	G-1-09	Marly limestone	Reddish brown to light brown marly limestone	49.35 to 50.00	2.52	4.52	1.80	33.35	27.113	39.39	1.20
51	G-1-10	Marly limestone	Reddish gray marly limestone	54.50 to 54.85	2.50	4.60	1.84	31.30	27.918	32.31	1.28
52	G-1-11	Marly limestone	Same as above	59.00 to 59.60	2.53	4.02	1.59	33.50	26.999	37.92	1.34
53	G-1-13	Marly limestone	Fresh reddish brown to light brown marly limestone	69.50 to 70.00	2.52	4.94	1.55	29.38	25.708	37.09	1.25

**Table 10** Macroscopic description, depth, type, dry density, porosity (*n*), water absorption (*A<sub>w</sub>*), DNPR, UCS, Schmidt hammer rebound, and point load index of Tang Tizab tunnel samples

Sample no.	Sample serial	Rock type	Sample description	Depth (m)	Density (kg/cm <sup>3</sup> )	<i>n</i> (%)	<i>A<sub>w</sub></i> (%)	UCS (MPa)	DNPR (N/mm)	<i>R<sub>L</sub></i>	<i>I<sub>s</sub></i> (50) (MPa)
54	1-01	Marly limestone	Highly weathered, jointed greenish gray marly limestone	18.00 to 18.30	2.26	7.91	2.38	13.70	10.160	28.73	–
55	1-03	Marly limestone	Light gray marly limestone	22.90 to 23.34	2.40	7.29	2.68	40.00	32.171	38.91	1.80
56	2-02	Marl	Highly weathered, jointed gray marl	18.55 to 18.87	2.42	5.34	2.67	37.85	30.270	46.05	1.70
57	2-03	Limestone	Highly weathered, jointed greenish light gray limestone	20.37 to 20.90	2.26	6.86	2.65	17.30	12.208	29.05	0.81
58	2-10	Marl	Gray marl	65 to 65.36	2.40	5.14	2.14	38.20	31.118	39.32	1.73
59	2-15	Marl	Faintly jointed gray marl	92.00 to 92.45	2.40	5.09	2.11	39.33	30.970	49.22	1.79
60	3-02	Marly limestone	Light gray marly limestone	–	2.43	3.79	1.48	40.00	33.038	49.91	1.85
61	3-03	Marly limestone	Same as above	–	2.41	3.25	1.26	37.10	33.067	44.21	1.31
62	3-08	Limestone	Light yellow limestone	–	2.37	3.62	1.41	29.22	24.063	33.94	1.26
63	3-09	Limestone	Same as above	–	2.40	3.84	1.50	38.00	34.016	46.38	1.69
64	4-13	Marl	Weathered dark gray marl	23.55 to 24.00	2.35	7.14	3.04	17.30	16.304	28.98	0.86
65	4-14	Limestone	Faintly weathered dark gray limestone	114.15 to 114.50	2.26	5.30	2.21	29.04	27.019	37.72	1.18

## References

- ASTM Standard A231/A231M (2010) Standard specification for chromium-vanadium alloy steel spring wire. doi:10.1520/A0231\_A0231M-10, [www.astm.org](http://www.astm.org)
- ASTM Standard A304 (2011) Standard specification for carbon and alloy steel bars subject to end-quench hardenability requirements. doi:10.1520/A0304-11, [www.astm.org](http://www.astm.org)
- ASTM Standard A681 (2008) Standard specification for tool steels alloy. doi:10.1520/A0681-08, [www.astm.org](http://www.astm.org)
- ASTM Standard D5731 (2008) Standard test method for determination of the point load strength index of rock and application to rock strength classifications. Doi: 10.1520/D5731-08, [www.astm.org](http://www.astm.org)
- Aydan Ö, Watanabe S, Tokashiki N (2008) The inference of mechanical properties of rocks from penetration tests. In: Proceedings of the 5th Asian Rock Mechanics Symposium (ARMS5), Tehran, Iran, vol. 1, pp. 213–220
- Aydin A, ISRM (2008) Suggested method for determination of the Schmidt hammer rebound hardness: revised version. Int J Rock Mech Mining Sci. doi:10.1016/j.ijrmms.2008.01.020
- Bahrami M, Parvanehnezhad Shirazi M (2010) Microfacies and sedimentary environments of Gurpi and Pabdeh formations and the type of Mesozoic–Cenozoic boundary in Fars province, Iran. J Appl Geol Winter 5(4):330–335
- Cevik A, Sezer EA, Cabalar AF, Gokceoglu C (2011) Modelling of the uniaxial compressive strength of some clay-bearing rocks using neural network. Appl Soft Comput 11(2):2587–2594
- Erguler ZA, Ulusay R (2009) Water-induced variations in mechanical properties of clay-bearing rocks. Int J Rock Mech Min Sci 46(2):355–370
- Gokceoglu C, Aksoy H (2000) New approaches for the characterization of clay-bearing, densely jointed and weak rock masses. Eng Geol 58(1):1–23
- Gokceoglu C, Ulusay R, Sonmez H (2000) Factors affecting durability of the weak and clay-bearing rocks selected from Turkey with particular emphasis on the influence of the number of drying and wetting of cycles. Eng Geol 57(3–4):215–237
- Humboldt Mfg Corporation (2003) Soil penetrometer: model H-4200 product manual. IL, USA
- Ismail A, Al-Juboury A (2009) The Upper Miocene Injana (Upper Fars) formation of Iraq: insights on provenance history. Arab J Geosci 2:337–364. doi:10.1007/s12517-009-0045-1

- ISRM (2007) The complete ISRM suggested methods for rock characterization, testing and monitoring: 1974–2006. Suggested methods prepared by the Commission on Testing Methods, International Society for Rock Mechanics, Ulusay R, and Hudson JA (eds.), compilation arranged by the ISRM Turkish National Group, Ankara, Turkey, 628 p
- Maruto Corporation (2006) Penetrometer for soft rock: model SH-70 instruction manual. Tokyo, Japan
- Minaeian B, Ahangari A (2011) Estimation of uniaxial compressive strength based on P-wave and Schmidt hammer rebound using statistical method. Arab J Geosci. doi:10.1007/s12517-011-0460-y
- Ngan-Tillard DJM, Engin HK, Verwaal W, Mulder A, Ulusay R, Erguler ZA (2012) Evaluation of micro-structural damage caused by needle penetration testing. Bull Eng Geol Environ 71:487–498. doi:10.1007/s10064-012-0430-y
- Ngan-Tillard DJM, Verwaal W, Maurenbrecher PM, Paassen LA van (2009) Microstructural degradation of Maastrichtian limestones. In: Proceedings of Eurock 2009, Engineering in Difficult Ground Conditions Soft Rocks and Karst Leiden, CRC Press, pp. 321–326
- Ngan-Tillard DJM, Verwaal W, Mulder A, Engin HK, Ulusay R (2011) Application of the needle penetration test to a calcarenite, Maastricht, the Netherlands. Eng Geol 123:214–424
- Potter PE, Maynard JB, Pryor WA (1980) Sedimentology of shale. Springer, New York
- Saket A (2006) Sedimentary rocks of Iran, Department of Geology, National Geosciences' Database of Iran (in Persian). <http://www.ngdir.ir/GeoportInfo/PSubjectInfoLists.asp?PID=598>
- Tavakoli-Shirazi S et al (2012) Evaluation of Cretaceous–Paleogene boundary based on calcareous nannofossils in section of Pol Dokhtar, Lorestan, southwestern Iran, Pre-Permian uplift and diffuse extensional deformation in the High Zagros Belt (Iran): integration in the geodynamic evolution of the Arabian plate. Arab J Geosci. doi:10.1007/s12517-012-0542-5
- Ulusay R, Erguler ZA (2007) Estimation of uniaxial compressive strength of clay-bearing weak rocks using needle penetration resistance. In: Ribeiro e Sousa L, Olalla C, Grossmann N (eds) The second half century of rock mechanics, 11th Congress of the International Society for Rock Mechanics. Taylor and Francis, London, Chapter 57, print ISBN: 978-0-415-45084-3, ebook ISBN: 978-0-415-88954-4
- Ulusay R, Gokceoglu C (1997) The modified block punch index test. Can Geotech J 34:991–1001